physica status solidi a
www.pss-a.com

$InAs_{0.7}Sb_{0.3}$ Bulk Photodiodes Operating at Thermoelectric-Cooler Temperatures

Q1 Natalya D. Il'inskaya Q2, Sergey A. Karandashev, Al'bert A. Lavrov, Boris A. Matveev,* Maxim A. Remennyi, Nicolay M. Stus', and Anna A. Usikova

Current–voltage and photoelectrical characteristics of $InAs_{0.7}Sb_{0.3}$ photodiodes grown onto InAs substrates are investigated in the interval of 212–330 K, i.e., the "thermoelectrical temperature range." The impacts of mesa diameter, buffer layer thickness, and cooling on the zero-bias resistance and spectral responsivity are described and analyzed. At low temperatures, the dynamic zero-bias resistance dominat the serial one, resulting in the specific detectivity at 6.5 μm and at $T = 233$ K being as high as $3.2 \cdot 10^8$ cm $\cdot$ Hz$^{1/2}$ $\cdot$ W^{-1} for a flat-plate photodiode.

1. Introduction

CdHgTe and InAsSb alloys have been traditionally used for many years as "bulk" absorbing layers in barrier and conventional mid-IR photodiodes (PDs) that have found applications in gas sensing,[1] IR thermometry,[2] and thermal imaging. Both alloys have a specific band structure that, despite the misfit dislocations formed during the growth on lattice mismatched substrates, allows for p-n structures with a low dark current and high quantum efficiency (see, e.g., Refs. [3–8]). For InAsSb-based structures, the above property is believed to be enabled by their unique property of producing electronic states above the conduction band, thereby suppressing the Shockley–Read–Hall recombination processes.[9,10] There is thus a good chance for manufacturing efficient PDs for radiation detection at wavelengths exceeding 6 μm by using lattice mismatched substrates, e.g., InAs substrates for the $InAs_{1-x}Sb_x$/InAs ($x > 0.2$, $\Delta a/a > 0.015$) heterostructure PDs. In certain cases, the $InAs_{1-x}Sb_x$/InAs structures are beneficial with respect to $InAs_{1-x}Sb_x$/GaSb structures because the former offer narrow bandwidth when illuminated from a side of the InAs substrate that cuts off radiation with wavelengths shorter than ≈3 μm. This makes InAs-based PDs "blind" to high-power medical lasers operating in the 2 μm range and thus allows simultaneous efficient delivery of high power through a fiber and precise detection of thermal radiation intensity and temperature measurements of the fiber tip performed in the 3–5 μm spectral range.

In this paper, we study $InAs_{0.7}Sb_{0.3}$ PDs grown onto InAs substrates, with an emphasis on an impact of mesa diameter, buffer layer thickness, and cooling on the zero-bias resistance and spectral responsivity values mainly in the temperature range of 212–330 K, usually referred to as the "thermoelectrical temperature range."

2. Experimental Methods and Sample Description

Shown in **Figure 1** are the chemical composition, interpolated energy gap $E_g^{300\,K}$(X,Y), and lattice constant mismatch ($\delta a/a$) of the $InAs_{1-x-y}Sb_xP_y$ alloy versus distance in a typical structure grown onto InAs substrate using a liquid-phase epitaxy method. The heterostructures with a 4–9 μm thick n-InAsSb buffer layer, a 3 μm thick n-InAsSb active layer, and a 3 μm thick P-InAsSbP(Zn) contact layer were processed using standard optical photolithography into rectangular flip-chip PDs. The PD chips of design described elsewhere[11] include an ≈100 μm thick n-InAs substrate, a circular broad metal anode on top of 35–250 μm wide circular active areas (mesas) with an unpassivated sidewall and a "horse shoe" metal cathode on the n-InAs substrate. Usually, there is sufficient spatial redistribution of radiation in flip-chip PDs[11]; thus, for the sake of the adequate optical area/responsivity evaluation, some PDs chips were additionally equipped with an opaque diaphragm with known open area or a hyperhemispherical Si immersion lens (Ø = 3.5 mm) glued onto the InAs substrate via a layer of chalcogenide glass with $n = 2.4$.

Figure 2(a) demonstrates room temperature (RT) heterostructure (wafer) transparency and electroluminescence (EL) and negative luminescence (NL) spectra both peaked at the photon energy of 180 meV, which is quite close to the $InAs_{0.7}Sb_{0.3}$ interpolated energy gap. L–I characteristics for both NL and EL operation modes (see Figure 2(b)) were almost linear, with a peak power of 3 μW at a forward current of I = 1 A (0.003 mW A^{-1}) at RT for the diode with the immersion lens. The latter value is

N. D. Il'inskaya, S. A. Karandashev, A. A. Lavrov, B. A. Matveev, M. A. Remennyi, N. M. Stus', A. A. Usikova
Ioffe Institute
26 Politekhnicheskaya, St. Petersburg 194021, Russian Federation
E-mail: ioffeled@mail.ru

A. A. Lavrov, N. M. Stus'
IoffeLED, Ltd.
26 Politekhnicheskaya, St. Petersburg 194021, Russian Federation

The ORCID identification number(s) for the author(s) of this article can be found under https://doi.org/10.1002/pssa.201700694.

DOI: 10.1002/pssa.201700694

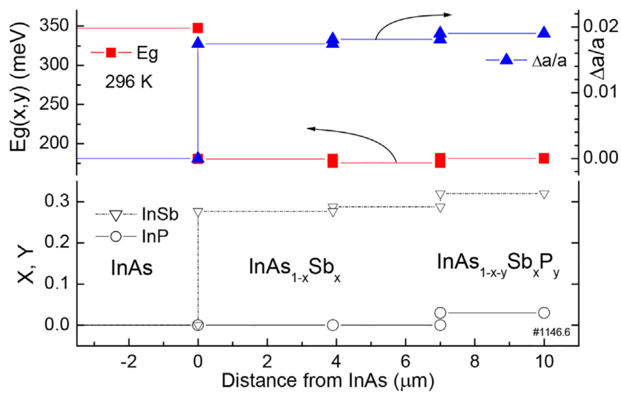

Figure 1. Mole fraction of InSb (X, ▽), InP (Y, ○) and simulated energy gap $E_g(X,Y)$ (■) and lattice mismatch with the InAs substrate ($\Delta a/a$, ▲) at room temperature versus distance in $InAsSb_{0.3}$ PD.

close to the power of the uncoated $InAsSb_{0.44}$ "barrier LEDs" with similar spectral characteristics when cooled down to 77 K in Ref. [12].

3. Results and Discussion

Figure 3 shows the "raw data" zero-bias resistance-area product ($R_0A = A \times dU/dI$) at RT as a function of mesa diameter D_m. As seen from the data in Figure 3, the R_0A product progressively decreases and conductivity increases as the PD lateral dimensions approach zero, indicating the presence of both bulk and surface leakage currents. The leakage current density was evaluated in a manner similar to that presented in Ref. [13], that is, from the dependence of a total dark current on mesa diameter. The corresponding data together with best fit curves presenting the simulated bulk $I_{p\text{-}n}$, the surface leakage $I_{surf.}$, and the total ($I_{p\text{-}n} + I_{surf.}$) currents at $U = -0.1$ V and $U = -0.2$ V are shown in **Figure 4**. As seen from Figure 4, the surface leakage current ($J_{surf.} = 0.1$ A cm^{-1} at $U = -0.1$ V) dominates the bulk one starting at mesa diameter less than ≈17 μm.

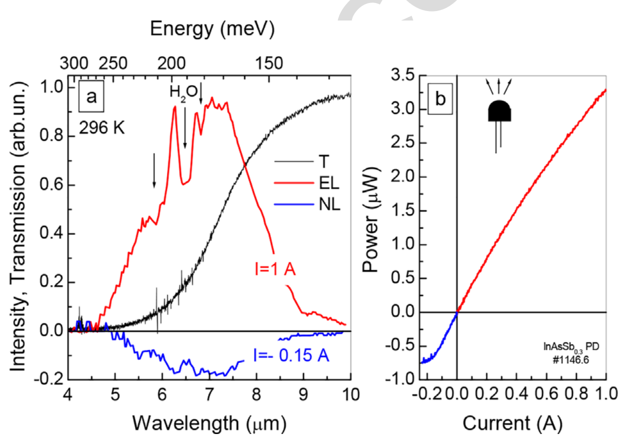

Figure 2. Room temperature EL and NL spectra together with the p–n structure transmission (a) and the L–I characteristic of the immersion lens PDs (b).

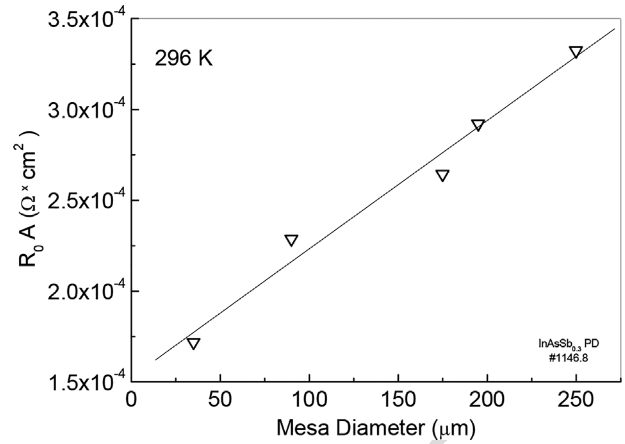

Figure 3. "Raw data" zero-bias resistance-area product (R_oA) versus mesa diameter D_m.

In general, an RT serial resistance R_s in narrow gap structures of a large lateral size is usually much greater than the dynamic p–n junction resistance, resulting in a nearly linear I–V characteristic for most forward-bias voltages $U_{forw.}$ (see, e.g., Ref. [14]). In such cases the I–V characteristic relative solely to the p–n junction properties could be obtained by extracting the voltage drop across the serial resistance in the following manner: $U_{p\text{-}n} = U_{forw.}\text{-}R_sI$, where $U_{p\text{-}n}$ is understood as a voltage across the p–n junction, and $R_s = dU_{forw}/dI$ at $U_{forw.} > 0.1$ V. Shown in **Figure 5** are the I–$V_{p\text{-}n}$ characteristics of the p–n junction in a 195 μm wide PD with $R_s \approx 1\,\Omega$ measured at several temperatures achievable by a 2-stage thermoelectric cooling. As shown in Figure 5, the I–$V_{p\text{-}n}$ characteristics at 212, 233, 256, 273, and 295 K adequately meet the modified Shockley formula $I = I_o \cdot [\exp(eU_{p\text{-}n}/\beta kT)\text{-}1]$, where e is the elementary charge, β is the ideality factor, k is the Boltzmann constant, and T is the temperature. The ideality factor β ranged from unity at $T = 295$ K

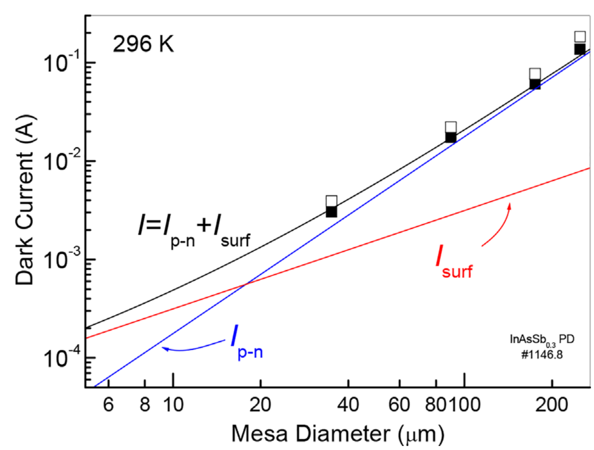

Figure 4. Total diode dark current at $U = -0.1$ (■) and -0.2 V (□) (b) in $InAsSb_{0.3}$ PDs at room temperature. The lines present the simulated bulk ($I_{p\text{-}n} = J_{p\text{-}n} \times \pi \times (D_m/2)^2$, $J_{p\text{-}n} = 56$ A cm^{-2}) and surface leakage ($I_{surf.} = J_{surf.} \times \pi \times D_m$, $J_{surf.} = 0.1$ A cm^{-1}) currents as well the sum of the above two currents ($I_{p\text{-}n} + I_{surf.}$) at $U = -0.1$ V.

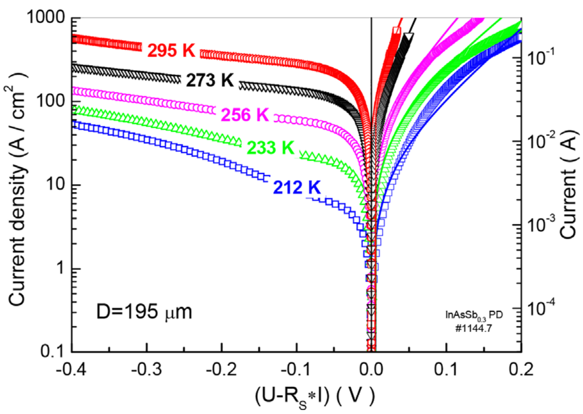

Figure 5. Dark current in $InAsSb_{0.3}$ PDs with an 8.8 μm thick buffer layer versus bias applied to the p–n junction $U_{p\text{-}n}$ at 212, 233, 256, 273, and 295 K. Solid lines represent the modified Shockley function.

to 3 at $T = 212$ K, indicating the dominance of the diffusion current near RT and probably the dominance tunneling at 212 K, respectively.

The prevalence of the diffusion current over other current types near RT is also supported by an analysis of the temperature dependence of the p–n junction zero-bias resistance-area product defined as $R_{p\text{-}n}A = \beta kTA/eI_o$, where e is the electron charge, and I_o is the "saturation current" parameter derived from the best fit of the above Shockley formula and experimental data in Figure 5. Indeed, the activation energy of an exponential growth of the $R_{p\text{-}n}A$ value near RT ($E_a = 234$ meV, see the Arrhenius plot in **Figure 6**) was close enough to the expected energy gap value $E_g(x,y) = 175$ meV (see data presented in Figure 1). The $R_{p\text{-}n}A$ values at $T = 250$–300 K appeared higher than R_oA published by Razeghi[3] for the InAsSb/InSb heterostructure PDs with nearly similar spectral response; in addition, at RT, the $R_{p\text{-}n}A$ value is not far from the expectations based on simulations made by Wróbel in Ref. [15].

When comparing $InAs_{0.7}Sb_{0.3}$ PDs with other detector types, note that in some cases, the R_oA or $R_{p\text{-}n}A$ value does not provide adequate performance characterization. For example, barrier detector current responsivity at small bias usually approaches zero; as a result, normally, the figure of merit is the dark current at a curtain bias and not the value of R_oA. The 233 K dark current value J_{dark} in our PDs was several times smaller than that in $InAsSb_{0.4}$ barrier photodiodes at $U = -0.45$ V with similar spectral response[8,9] and was ≈10 times higher than the values derived from the "Rule 07" directives.[16] Shown in Figure 6 is the temperature dependence of the J_{dark}/T^3 ratio at biases of −0.1 and −0.4 V, where the term T^3 accounts for the temperature dependence of the density of states in the expression for the diffusion current density.[8] The activation energy of the J_{dark}/T^3 exponential dependence at $U = -0.1$ V and $T > 230$ K was close to that of the $R_{p\text{-}n}A$, that is, it was approximately two times higher than that expected for a PD with dominant generation-recombination current.

It is generally anticipated that the dark current in lattice-mismatched PD structures declines with increasing buffer layer thickness (see, e.g., Refs. [17,18]). In our case, however, the above "rule of thumb" was not very well pronounced, as only minor PD zero-bias resistance and sensitivity enhancement in PDs with thick buffer could be traced from the data in **Figure 7**(b) and (c). In contrast, a remarkable change in spectral response was observed: the relative responsivity at short waves progressively increased as the buffer layer thickness (t) decreased via the collection efficiency enhancement in "thin buffer" structures, e.g., from 0.3 at $t = 9$ μm up to 0.8 at $t = 4$ μm ($\lambda = 5$ μm) (see Figure 7(a)). The responsivity dependence on t suggests that the hole diffusion length L_p and a distance between the InAs/InAsSb and the p–n junctions are of the same order. Draft evaluation provides values of $L_p^{300\,K} \approx 6$ μm, which are close to the estimations of the same parameter in n-InAsSb-based PDs given in Refs. [8,19,20] and approximately two times larger than that in Ref. [6].

The shortwave responsivity shoulder is obviously related to the n-InAs substrate transparency spectrum; the longwave

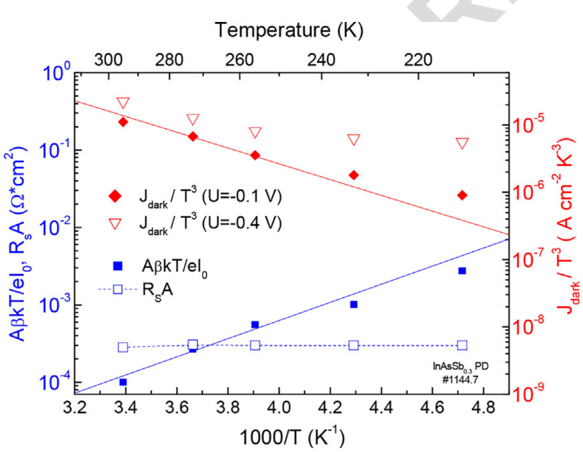

Figure 6. Zero-bias resistance–area product of the p–n junction ($R_{p\text{-}n}A$, ■) and serial resistance–area product (R_sA, □) versus reciprocal temperature for a 195 μm wide mesa PD with an 8.8 μm thick buffer layer (all at the left scale) and temperature dependence of the term J_{dark}/T^3 at a reverse bias of −0.1 V (◆) and −0.4 V (▽) (both using the right scale). Solid lines denote the exp(E_a/kT) and exp($-E_a/kT$) functions.

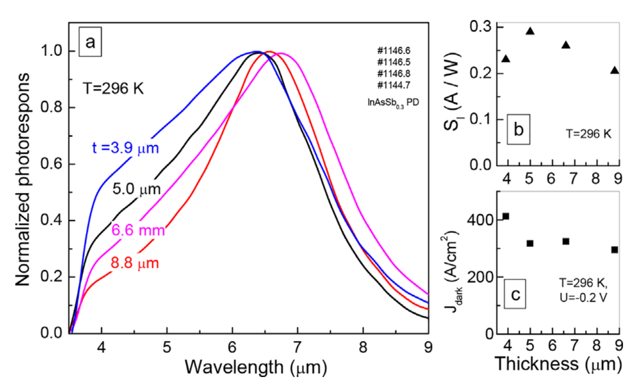

Figure 7. Room temperature normalized photoresponse spectra (a), peak sensitivity (b), and dark current at −0.2 V (c) versus buffer layer thickness (t) in $InAsSb_{0.3}$ PDs.

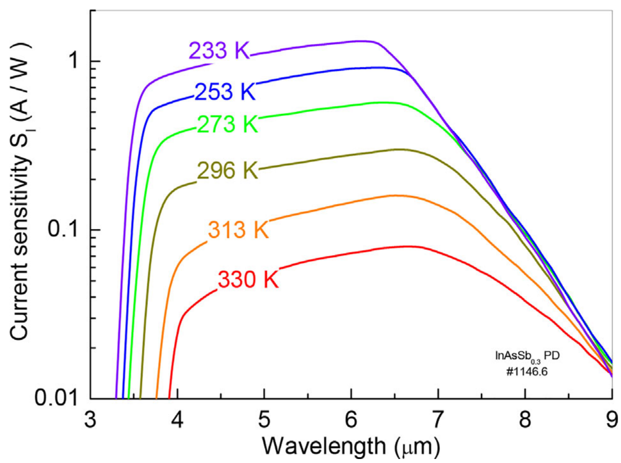

Figure 8. Photoresponse spectra of the PD with 3.9 μm thick buffer layer in the 233–330 K interval.

shoulder was temperature-sensitive with a $0.28\,\text{meV}\,\text{K}^{-1}$ temperature shift rate close to InAs energy-gap variation (see **Figure 8**). The responsivity near the peak wavelength exhibited nice growth upon cooling of the PD, as shown in Figure 8 and 9; this result most likely highlights the prevalence of the p–n junction resistance over R_s at low temperatures. At 233 K, the 195 μm wide mesa PD zero-bias resistance-area product R_oA and responsivity S_I at a wavelength of 6.5 μm were $0.0015\,\Omega\,\text{cm}^2$ and $1\,\text{A}\,\text{W}^{-1}$, respectively, which are higher than those in "commercial" CdHgTe detectors mounted onto a 2-stage thermoelectric cooler (see, e.g., Ref. [21]). Coherently, the simulated Johnson noise limited specific detectivity is also higher than that in Ref. [21] (see **Figure 9**) and at $\lambda = 6.5\,\mu\text{m}$ amounts to $3.2 \cdot 10^8\,\text{cm} \cdot \text{Hz}^{1/2} \cdot \text{W}^{-1}$ for a bare chip PD. Incorporation of a hyperhemispherical immersion Si lens ($\text{Ø} = 3.5\,\text{mm}$) increases the $D^*_{6.5\,\mu\text{m},\ 233\,\text{K}}$ up to $4.3 \cdot 10^9\,\text{cm} \cdot \text{Hz}^{1/2} \cdot \text{W}^{-1}$, making $\text{InAsSb}_{0.3}$ PDs superior to the commercial PDs, at least at wavelengths of ≈6.5 μm.

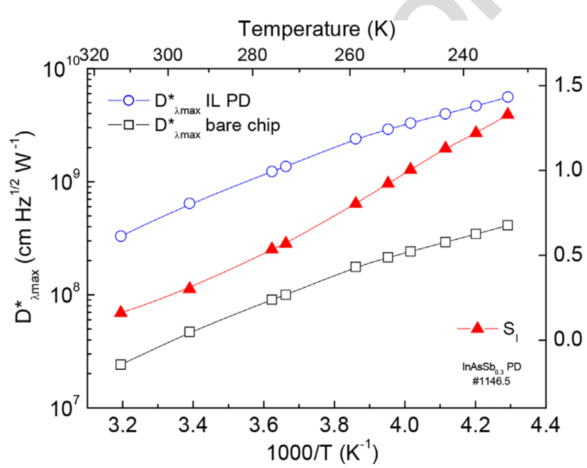

Figure 9. Specific detectivity D^* for bare chip (□) and immersion lens (○) PDs (left scale) and responsivity (right scale, ▲) at maximum versus temperature in a 195 μm wide bare chip $\text{InAsSb}_{0.3}$ PD with 5 μm thick buffer layer.

4. Conclusions

$\text{InAsSbP/InAsSb}_{0.3}$ p–n heterostructures grown onto InAs substrates demonstrated diffusion-limited current at near room temperature and tunnel current at 212–250 K with predominantly series resistance in the temperature range of 270–300 K. The zero-bias p–n junction resistance-area product was close to the theoretical estimations, and the specific detectivity at 233 K achievable by a 2-stage thermoelectric cooler amounted to remarkable values of $D^*_{6.5\,\mu\text{m}} = 3.2 \cdot 10^8$ and $4.3 \cdot 10^9$ Jones for the 195 μm wide bare chip and immersion lens PDs ($\text{Ø} = 3.5\,\text{mm}$), respectively.

Acknowledgments

We thank A.S. Petrov (Open Society Central Research Institute "Electron") for helpful discussions and the Shared Service Center "Material Science and Diagnostics for Advanced Technologies" for performing the X-ray microanalysis. The work performed at *IoffeLED, Ltd.* has been supported by the RF state program "Development of fabrication processes for semiconductor materials for use in matrix photodetectors and thermal vision," contract #14.576.21.0057 (ID: RFMEFI57614X0057).

Conflict of Interest

The[Q3] authors declare no conflict of interest.

Keywords

backside illuminated photodiodes, dark current, InAsSb photodiodes, infrared sensors, IR gas sensors, mid-IR detectors, pyrometry

Received: September 8, 2017
Revised: December 7, 2017
Published online:

[1] J. Hodgkinson, R. P. Tatam, *Meas. Sci. Technol*. **2013**, *24*, 012004.
[2] D. Zymelka, B. Matveev, S. Aleksandrov, G. Sotnikova, G. Gavrilov, M. Saadaoui, *IOP J. Flexible Printed Electron*. **2017**, *2*, 045006.
[3] M. Razeghi, *Eur. Phys. J. AP* **2003**, *23*, 149.
[4] V. M. Bazovkin, S. A. Dvoretsky, A. A. Guzev, A. P. Kovchavtsev, D. V. Marin, V. G. Polovinkin, I. V. Sabinina, G. Yu. Sidorov, A. V. Tsarenko, V. V. Vasil'ev, V. S. Varavin, M. V. Yakushev, *Infr. Phys. Technol*. **2016**, *76*, 72.
[5] N. Baril, A. Brown, P. Maloney, M. Tidrow, D. Lubyshev, Y. Qui, J. M. Fastenau, A. W. K. Liu, S. Bandara, *Appl. Phys. Lett*. **2016**, *109*, 122104.
[6] A. P. Craig, A. R. J. Marshall, Z.-B. Tian, S. Krishna, A. Krier, *Appl. Phys. Lett*. **2013**, *103*, 253502.
[7] D. Wang, D. Donetsky, G. Kipshidze, Y. Lin, L. Shterengas, G. Belenky, W. Sarney, S. Svensson, *Appl. Phys. Lett*. **2013**, *103*, 051120.
[8] Y. Lin, D. Wang, D. Donetsky, G. Kipshidze, L. Shterengas, L. E. Vorobjev, G. Belenky, *Semicond. Sci. Technol*. **2014**, *29*, 112002.

[9] P. J. P. Tang, C. C. Phillips, R. A. Stradling, *Semicond. Sci. Technol*. **1993**, *8*, 2135.
[10] A. D. Prins, M. K. Lewis, Z. L. Bushell, S. J. Sweeney, S. Liu, Y.-H. Zhang, *Appl. Phys. Lett*. **2015**, *106*, 171111.
[11] A. L. Zakgeim, N. D. Il'inskaya, S. A. Karandashev, A. A. Lavrov, B. A. Matveev, M. A. Remennyy, N. M. Stus', A. A. Usikova, A. E. Cherniakov, *Semiconductors* **2017**, *51*, 260.
[12] G. Belenky, D. Wang, Y. Lin, D. Donetsky, G. Kipshidze, L. Shterengas, D. Westerfeld, W. L. Sarney, S. P. Svensson, *Appl. Phys. Lett*. **2013**, *102*, 111108.
[13] P. J. Ker, A. R. J. Marchall, J. P. R. David, C. H. Tan, *Phys. Stat. Sol*. **2012**, *C9*, 310.
[14] J. D. Kim, S. Kim, D. Wu, J. Wojkowski, J. Xu, J. Piotrowski, E. Bigan, M. Razeghi, *Appl. Phys. Lett*. **1995**, *67*, 2645.
[15] J. Wróbel, R. Ciupa, A. Rogalski, Conf. *Infrared Technology and Applications XXXVI* (Orlando, Florida, USA, 5–9 April **2010**) *Proc. of SPIE 7660*, pp. 766033-1–766033-9.
[16] W. E. Tennant, *J. Electron. Mater.* **2012**, *39*, 1030.
[17] A. Krier, W. Suleiman, *Appl. Phys. Lett*. **2006**, *89*, 083512.
[18] G. R. Savich, D. E. Sidor, X. Du, C. P. Morath, V. M. Cowan, G. W. Wicks, Conf. *Nanophotonics and Macrophotonics for Space Environments VIII* (San Diego, California, USA, 17–21 August **2014**) *Proc. of SPIE 9226*, pp. 92260R-1–92260R-6.
[19] A. Soibel, C. J. Hill, S. A. Keo, L. Hoglund, R. Rosenberg, R. Kowalczyk, A. Khoshakhlagh, A. Fisher, D. Z.-Y. Ting, S. D. Gunapala, *Appl. Phys. Lett*. **2014**, *105*, 023512.
[20] G. Marre, B. Vinter, V. Berger, *Semicond. Sci. Technol*. **2003**, *18*, 284.
[21] www.vigo.com.pl.

ORIGINAL PAPER

Keyword

N. D. Il'inskaya, S. A. Karandashev,
A. A. Lavrov, B. A. Matveev,*
M. A. Remennyi, N. M. Stus',
A. A. Usikova 1700694

$InAs_{0.7}Sb_{0.3}$ Bulk Photodiodes Operating at Thermoelectric-Cooler Temperatures

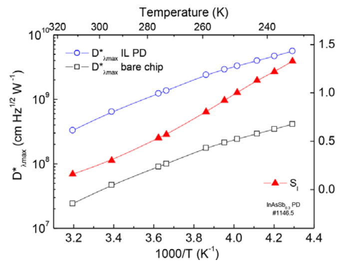

Low energy gap flip-chip photodiodes with $InAsSb_{0.3}$ absorbing layer have been fabricated. These photodiodes exhibit reasonably high values of specific detectivity and responsivity at 6.5 µm when cooled down to 233 K which is essential for many spectroscopic measurements including pyrometry and gas analysis.